How myristyltrimethylammonium bromide enhances biomass harvesting and pigments extraction from…

Article *in* Water Research · September 2017

DOI: 10.1016/j.watres.2017.09.036

CITATIONS
0

READS
109

7 authors, including:

Everett Eustance
Arizona State University
13 PUBLICATIONS **131** CITATIONS
SEE PROFILE

Chen Zhou
Arizona State University
31 PUBLICATIONS **210** CITATIONS
SEE PROFILE

Siqing Xia
Tongji University
164 PUBLICATIONS **2,597** CITATIONS
SEE PROFILE

Bruce Rittmann
Arizona State University
688 PUBLICATIONS **23,746** CITATIONS
SEE PROFILE

Water Research 126 (2017) 189–196

Contents lists available at ScienceDirect

Water Research

journal homepage: www.elsevier.com/locate/watres

How myristyltrimethylammonium bromide enhances biomass harvesting and pigments extraction from *Synechocystis* sp. PCC 6803

Yun Zhou [a, b], YenJung Sean Lai [a], Everett Eustance [a], Levi Straka [a], Chen Zhou [a], Siqing Xia [b, *], Bruce E. Rittmann [a, **]

[a] Biodesign Swette Center for Environmental Biotechnology, Arizona State University, Tempe, AZ 85287-5701, United States
[b] State Key Laboratory of Pollution Control and Resource Reuse, College of Environmental Science and Engineering, Tongji University, Shanghai, 200092, China

ARTICLE INFO

Article history:
Received 13 July 2017
Received in revised form
14 September 2017
Accepted 20 September 2017
Available online 21 September 2017

Keywords:
Synechocystis
Harvesting and extraction
Cationic surfactant
Mechanisms
Cyanobacteria

ABSTRACT

Myristyltrimethylammonium bromide (MTAB) is a cationic surfactant used to improve biomass harvesting and pigment extraction form microalgae, but the mechanisms underlying its effectiveness are poorly defined. We document the mechanisms for enhanced harvesting and pigment extraction for the cyanobacterium *Synechocystis* sp. PCC 6803 using measurements from flow cytometer, zeta potential, release of soluble components, and microscopy. Harvesting efficiency increased as the MTAB/Biomass dose increased from 0 to 40%. A low MTAB dose ($\leq$ 8%) mainly brought about coagulation and flocculation, which led to aggregation that improved harvesting, but 40% MTAB had the highest harvesting efficiency, 62%. Adding MTAB above a MTAB/Biomass dose of 8% also increased cell-membrane permeability, which allowed the solvent (ethyl acetate) to pass into the cells and resulted in a large increase in extraction efficiency of pigments: An MTAB/Biomass ratio of 60% for 180 min achieved the highest extraction efficiencies of chlorophyll and carotenoids, 95% and 91%, respectively. Combining harvesting and extraction performances with results from flow cytometry, zeta potential, release of soluble components, and microscopy lead to the following mechanistic understandings. MTAB dose from 8% to 40% solubilized EPS, which lowered the biomass's negative charge, but caused breakup of the large aggregates. An increase of cell permeability also in this stage allowed ethyl acetate to pass into the cells and achieve better pigment extraction. MTAB >40% led to cell lysis and a large increase in soluble organics, but complete cell lysis was not required to achieve the maximum extraction efficiency. The MTAB/Biomass % ratio for optimizing harvest efficiency and pigment extraction lay in the range of 40%–60%.

1. Introduction

Microalgae have enormous potential to be sustainable feedstock for numerous bioproducts (Ruiz et al., 2016), such as lipids, proteins, carbohydrates, and high-value compounds based on chlorophyll, carotenoids, antioxidants, and sterols (Gilbert-López et al., 2015; Oswald and Golueke, 1960; Pittman et al., 2011). Today, the production of high-value products is considered to be essential for making microalgae systems profitable (Ruiz et al., 2016). Major challenges for utilizing microalgae lie in harvesting the biomass and extracting intracellular products (Vandamme et al., 2013). Integrating biomass harvesting and product extraction into one simple step offers an opportunity to lower financial and energy costs in a major way (Lai et al., 2016b; Seo et al., 2016).

Coagulation and flocculation are important mechanisms in biomass harvesting (Lai et al., 2016a; Wan et al., 2015). Flocculation typically utilizes long-chain polyelectrolytes (usually cationic) to improve the biomass harvesting by linking the particles together (Hermansson, 1999; Magara et al., 1976). Coagulation promotes flocculation by decreasing the zeta potential of the suspended particles (Biggs et al., 2000; Ries and Meyers, 1968). Among the

Abbreviations: MTAB, Myristyltrimethylammonium bromide; EPS, Extracellular polymeric substances; FC, Flow cytometry; SG, SYTOX Green; NA, Nucleic acid; OD_{730}, The optical density at 730 nm; EA, Ethyl acetate; FI, Fluorescent intensity; DW, Dry weight; PCOD, Particulate chemical oxygen demand; BSA, Bovine serum albumin; SOC, Soluble organic compounds; SP, Soluble protein; SC, Soluble carbohydrate; SL, Slope; FSC, Forward scatter; SSC, Side scatter.

* Corresponding author.
** Corresponding author.
E-mail addresses: siqingxia@tongji.edu.cn (S. Xia), Rittmann@asu.edu (B.E. Rittmann).

https://doi.org/10.1016/j.watres.2017.09.036
0043-1354/

options are surfactants such as myristyltrimethylammonium bromide (MTAB, $C_{17}H_{38}NBr$), which has an alkyl-chain length of C14 and a quaternary-ammonium cation (Lai et al., 2016a, 2016b; Seo et al., 2016).

Extracellular polymeric substances (EPS) play important roles in biomass aggregation (Liu et al., 2007; Zhang et al., 2016). On the one hand, EPS contains carboxylic (≡X-COOH) and phosphoryl (≡X-PO_4H) groups (Schwarz and Rittmann, 2007; Zhou et al., 2016b, 2017a) that are negatively charged at slightly acidic to alkaline conditions (Zhou et al., 2017a). Un-neutralized, the negative functional groups prevent aggregation. Having a quaternary-ammonium cation, MTAB can neutralize the negative charges, and its long alkyl chain can serve as an inter-particle bridge; both aspects enhance aggregation (Sengco et al., 2001). On the other hand, if too much MTAB is added, its surfactant effect can dominate, resulting in the release of EPS from the cells and deflocculation (Lu et al., 2017; Schott et al., 1982).

Another feature of MTAB is that, because its linear hydrocarbon group is hydrophobic, MTAB can form micelles that are effective for extracting hydrophobic components from the cells and also can lead to cell lysis and release of intracellular compounds (Zhou et al., 2016c, 2017b). These effects can play important roles in the extraction of intracellular components, such as pigments.

The mechanisms affecting aggregation and product extraction depend on the MTAB concentration. For example, a previous study (Lai et al., 2016b) found that a 20% MTAB/Biomass ratio achieved the highest harvesting efficiency (due to aggregation) of *Chlorella*, but a 44% ratio achieved the highest extraction efficiency for fatty acid methyl esters (FAME).

Flow cytometry (FC) is a powerful tool to determine physical and chemical characteristics of single particles, including intact cells and cellular debris after lysis (Hyka et al., 2013). FC can be used to achieve two goals (Collier, 2000; Sheng et al., 2011; Vermes et al., 2000; Zhou et al., 2016a; Zipper et al., 2004): (1) characterizing cell features, such as cell size and granularity and cell membrane integrity; and (2) cell sorting according to size or a metabolic feature, such as autofluorescence emitted from chlorophyll, a pigment present in all photoautotrophic microalgae.

FC combined with SYTOX Green (SG) dye is commonly used for the characterization of cell features (Sheng et al., 2011; Zhou et al., 2016a; Zipper et al., 2004). SG is an unsymmetrical cyanine dye that binds strongly with nucleic acid (NA) (Lebaron et al., 1998). Because of its large molecular size, SG cannot penetrate an intact cell membrane (Roth et al., 1997; Zipper et al., 2004), and the emitted fluorescence is due only to NA in the EPS of intact biomass. However, when cells are compromised, such as by lysis, intracellular DNA can be complexed by SG. Since the concentration of intracellular NA is much higher than NA in EPS, the fluorescence emitted by SG complexed to released intracellular NA is much larger than SG complexed solely to extracellular NA (Roth et al., 1997; Sheng et al., 2011). Thus, FC with SG can sensitively differentiate whether or not cells have been lysed. As an example, previous study (Zhou et al., 2016a) used flow cytometry to evaluate thermal extraction of EPS from *Synechocystis* sp. PCC 6803 and showed that lysis was minimal during a 20-min thermal extraction as long as the temperature was less than 60 °C.

Although surfactants are used for biomass harvesting and pigment extraction, the mechanisms are not well understood. In this study, we use FC with SG, zeta-potential measurements, release of soluble components, and microscopy to comprehensively monitor how MTAB enhances biomass harvesting and pigments extraction. We show that adding just enough MTAB for complete EPS removal, but with minimal cell lysis, achieves the maximum harvesting efficiency by coagulation and flocculation. Furthermore, pigment extraction is enhanced by adding MTAB to a concentration that achieves an increase in cell-membrane permeability that allows solvent to diffuse into the cells, but does not lyse the cells completely.

2. Materials and methods

2.1. Chemicals and Synechocystis sp. PCC 6803 samples

Myristyltrimethylammonium bromide (MTAB) was obtained from Sigma-Aldrich (St. Louis, MO). A stock solution of MTAB with a concentration of 20 g/L was prepared by dissolving analytical grade of MTAB into deionized (DI) water.

Wild-type *Synechocystis* sp. PCC 6803 (hereafter *Synechocystis*) was grown in 1-L Erlenmeyer flasks with a working volume of 500 mL, utilizing standard BG-11 medium (Rippka et al., 1979) and bubbled with air filtered through a 1.0-μm air filter (Pall, Port Washington, NY, USA) at a flow rate of about 0.1 L/min. The culturing conditions were: temperature of 30 °C, maintained by 3 × 12-W automated-air fans (Nguyen and Rittmann, 2016); incident light intensity of 276 $\mu E/m^2.s$, provided from T5 fluorescent plant grow lamps (Envirogro Hydrofarm, USA); and pH of 8.0 maintained using a pH-Stat that automatically sparged pure CO_2 when the pH was higher than 8.01 (Nguyen and Rittmann, 2015). Prior to inoculation, the flasks and the BG-11 medium were sterilized by autoclaving, and the pH probe was sterilized using 75% ethanol. After 5 days of cultivation, the optical density at 730 nm (OD_{730}) of the culture rose to ~ 2.3 and biomass dry weight to ~ 650 mg/L. After 5 days of growth, the biomass was collected for testing. In order to eliminate the effect of divalent metal ions (Ca^{2+} and Mg^{2+} in the standard BG-11) on biomass harvesting (Ayed et al., 2015; Li et al., 2017) or extraction, we centrifuged the culture at 4000 rpm at 4 °C for 10 min and then replaced the supernatant using the same volume of DI water. Table 1 summarizes characteristics of the *Synechocystis* samples used for the biomass harvesting and products extraction.

2.2. Biomass harvesting

The biomass-harvesting efficiency was evaluated by measuring culture OD_{730} over time. We mixed 10 mL of a *Synechocystis* sample with MTAB in 15-mL polypropylene centrifuge tubes (BD Falcon, VWR, USA), using the following mass ratios (MTAB mass/biomass dry weight, %): 0, 4, 8, 12, 20, 25, 30, 35, 40, 45, 50, 55, 60, 65, and 70. We mixed the samples by hand until the contents were well-mixed. During the harvesting period (up to 240 min), we withdrew duplicate 0.15-ml samples from the middle of the tube (Salim et al., 2011) and diluted them to 1.5 mL using DI water for a final OD_{730} below 1.0. We calculated the harvest efficiency using the following equation (Salim et al., 2011):

$$\textit{Harvesting efficiency}\ (\%) = \frac{OD_{730}(t_0) - OD_{730}(t)}{OD_{730}(t_0)} \times 100$$

where $OD_{730}(t_0)$ is the OD of the sample at time zero, and $OD_{730}(t)$ is the OD of the sample after t min.

2.3. Pigments extraction and SOC separation

The effects of MTAB on the efficiency of pigment extraction were evaluated using the wet-biomass-extraction method (Lai et al., 2016a). We mixed 10 mL of the prepared *Synechocystis* with MTAB each in 15-mL polypropylene centrifuge tubes (BD Falcon, VWR, USA) with the following mass ratios (MTAB mass/biomass dry weight, %): 0, 4, 8, 12, 20, 25, 30, 35, 40, 45, 50, 55, 60, 65, and 70. The slurries were mixed within an incubator (New Brunswick

Table 1
Characteristics of *Synechocystis* sp. PCC 6803 used in this study.

Parameter	Unit	Value
pH	–	8.0 ± 0.05
OD_{730} [a]	–	2.2 ± 0.2
DW [b]	mg/L	626 ± 4.3
PCOD [c]	mg COD/L	728 ± 13
Chlorophyll	mg/L	37 ± 3.4
Carotenoid	mg/L	19.8 ± 2.1
EPS [d]	mg COD/L	68.4 ± 5.3
Protein in EPS	mg COD/L	39.1 ± 3.5
Carbohydrate in EPS	mg COD/L	22.8 ± 2.5

[a] OD_{730} is the optical density at 730 nm.
[b] DW is the dry weight of biomass.
[c] PCOD is particulate chemical oxygen demand.
[d] EPS is extracellular polymeric substances.

Scientific, Enfield, CT) at 210 rpm and at room temperature (23.8 °C). After 3 h, we withdrew a 1-mL sample and mixed it with 3 mL of ethyl acetate (EA) solvent in 7.5-mL Pyrex disposable screw-cap culture tubes (13 × 100 mm). The mixtures of EA and biomass were vortexed at 3200 rpm for 1 min on Vortex-Genie 2 (Scientific Industries, USA) and then centrifuged at 4000 rpm for 5 min. We removed 2 mL of clear centrate for the assay of extractable chlorophyll and carotenoid.

To define the maximum extraction of chlorophyll and carotenoids (Gilbert-López et al., 2015), we mixed a 1-mL slurry sample containing 626 ± 4.3 mg/L of freeze-dried biomass (FreeZone Benchtop instrument (Labconco, MO, USA)) with 3 mL of Folch solvent (Chloroform: methanol = 2:1 v:v) in a 7.5-mL Pyrex disposable screw-cap culture tube. The mixture was subsequently shaken at 3200 rpm for 5 h on the Vortex-Genie 2 and then centrifuged at 4000 rpm and 23 °C for 10 min to separate the solids. We took out 2 mL of centrate for the assay of total chlorophyll and carotenoid.

We withdrew 4 mL of the MTAB-treated samples and centrifuged them at 4000 rpm and 4 °C for 15 min. We further centrifuged the centrate at 12000 rpm (Microfuge® 22 R Centrifuge, Beckman Coulter, CA, USA) and 4 °C for 10 min to ensure that all particles had been removed. The centrate was assayed for released protein and carbohydrate. Total EPS was extracted from *Synechocystis* biomass using a thermal method (Zhou et al., 2016a), briefly thermal treatment at 60 °C for 20 min and rapidly cooled the culture to room temperature (23.8 °C), and then filtered the culture through a 0.2-μm cellulose acetate membrane filter (Whatman, Germany). All of the samples were stored at 4 °C in a freezer (UGL3020A, Thermo Scientific, USA) prior to all analyses.

2.4. SYTOX Green staining and flow cytometry

We adapted an SG-staining and flow-cytometry approach (Sheng et al., 2011; Zhou et al., 2016a) to identify cell size, release of SOC, and cell lysis after MTAB treatment. We applied the fluorescent dye SG according to the manufacturer's guidelines (Invitrogen, Carlsbad, CA). After treatment for 3 h, we withdrew a 2-mL sample, mixed it with 1 μL SG, and then allowed the reaction to proceed for 15 min in the dark on a rocker mixer (Lab-Line, TX, U.S.). We used *Synechocystis* biomass without treatment or SG stain to zero the fluorescent intensity (FI).

2.5. Analytical methods

Sample OD_{730} was measured with a UV–vis BioSpec-mini spectrometer at 730 nm (Shimadzu Corp., Japan). Dry weight (DW) was quantified using the total suspended solids assay, Method 2540D in *Standard Methods* (Association, 1998) and DW was converted to particulate chemical oxygen demand (PCOD) assuming a conversion factor of 1.4 mg COD/mg DW (Rittmann and McCarty, 2001). We measured the protein in SOC with a QuantiPro BCA Assay Kit (Sigma-Aldrich, St. Louis, MO, U.S.) using bovine serum albumin (BSA) as the standard; BSA equivalents were converted to COD using a conversion factor of 1.4 mg COD/mg BSA (Bruce and Perry, 2001). The carbohydrate content in the SOC was assayed with the phenol-sulfuric acid method using glucose as the standard (Frølund et al., 1996), and it was converted from glucose equivalents to COD using a conversion factor of 1.07 mg COD/mg glucose (Rittmann and McCarty, 2001).

The concentrations of chlorophyll and carotenoid were measured with a spectrophotometer (Bio Cary 50 – Varian, USA) based on the characteristic absorbances of the pigments (Gilbert-López et al., 2015): 470 and 665 nm for chlorophyll and carotenoid, respectively. Standard curves are in Fig. S1.

The zeta potential was measured using a Zetasizer (Nano-ZS, Malvern) after the biomass was diluted to a manufacture-recommended concentration between 0.1 g/L and 1 g/L (Lai et al., 2016b).

Cell morphology of *Synechocystis* after treatment by the various MTAB doses were observed using an optical microscope (BX61, Olympus Corporation, Germany), and images were captured by a digital camera (DP70, Olympus Corporation, Germany).

2.6. Statistical analysis

For MTAB-treatment experiments, we used three tubes for each MTAB dose, and the sample in each tube was assayed one time for OD_{730}, chlorophyll, carotenoid, protein, and carbohydrate. Results are expressed as the mean and standard deviation of the three measured samples (mean ± SD). When presenting the results of *Synechocystis* cell morphology, light scattering, and the spectra from FC, we show one representative result for each sample. Statistical analysis with SPSS software for Windows (SPSS, Chicago, Illinois, USA) was used to identify the strength of the relationship between two parameters. The Pearson's correlation coefficient, R^2, was used to estimate the linear correlation between two parameters. Correlations were considered statistically significance at a 95% confidence interval ($P < 0.05$).

3. Results and discussion

3.1. Effects of MTAB dose on harvest efficiency

Fig. 1 shows the harvest efficiency of *Synechocystis* after treatment with MTAB at different MTAB/Biomass % ratios for the noted times, along with the harvest efficiency and zeta potentials of *Synechocystis* with the range of doses after MTAB treatment for 180 min. Fig. S2 presents the corresponding OD_{730} values. *Synechocystis* did not self-flocculate (harvest efficiency was ~0% with no added MTAB), but MTAB brought about coagulation and flocculation that enhanced biomass harvesting (Fig. 1(a)). Based on harvest efficiency, the MTAB/Biomass % ratio can be divided into three ranges: 0–40% (Range I), 40–55% (Range II), and 55–70% (Range III). Within Range I, the harvest efficiency dramatically increased with higher MTAB dose and continued to increase throughout the 240 min test (Fig. 1(a1)). Comparing results at 180 min, the harvest efficiency and zeta potential gradually increased with MTAB dose (Fig. 1(b) and (c)). In Range II, the harvest efficiency was higher than in Range I for up to about 180 min, but gradually decreased out to 240 min (Fig. 1(a2)). The best harvest efficiency achieved was 61.7 ± 2.4% using 40% MTAB/biomass and

180 min of contact time (Fig. 1(b)). In Range III, the harvest efficiency was lower than that achieved by the concentrations in Range II, even though the zeta potential increased to nearly 0 mV (Fig. 1(b) and (c)).

3.2. Effects of MTAB doses on pigment extraction

Fig. 2 presents the extraction efficiencies of chlorophyll and carotenoids from *Synechocystis* after treatment with MTAB at various MTAB/Biomass % ratios for 180 min; Fig. S3 presents the corresponding concentrations of chlorophyll and carotenoid. The extraction efficiencies for chlorophyll and carotenoid changed systematically with the MTAB/Biomass % ratio and can be grouped into the same three ranges as for harvest efficiency. In Range I (mass ratios of 0%–40%), the extraction efficiencies for chlorophyll and carotenoid dramatically increased with increasing MTAB dose, although the large increase was for a mass ratio $\geq$ 20%. In Range II (mass ratio from 40% to 55%), the extraction efficiencies for chlorophyll and carotenoid slowly increased approaching the maximum, and in Range III (mass ratios of 55%–70%) they remained stable. The maximum extraction efficiencies were 94.5 ± 3.6% and 91.4 ± 2.2% for chlorophyll and carotenoid, respectively, and they occurred with an MTAB/biomass ratio of 60% for the 180-min treatment, although the efficiencies were nearly the same for MTAB/Biomass ratios of 55%–70%.

3.3. Releasing soluble organic compounds

Fig. 3 shows the release of soluble protein (SP) and carbohydrate (SC) from *Synechocystis* after treatment with MTAB at the various MTAB/Biomass % ratios for 3 h. SP and SC changed systematically with MTAB/Biomass % ratio and can be grouped into two stages that differ from the ranges that describe harvesting and pigment extraction. In Stage I (from 0% to 35%), SP and SC increased steadily with increasing MTAB dose, and the concentration of SP + SC has a strong and nearly linear relationship ($R^2 = 0.996$, $P < 0.01$) with the

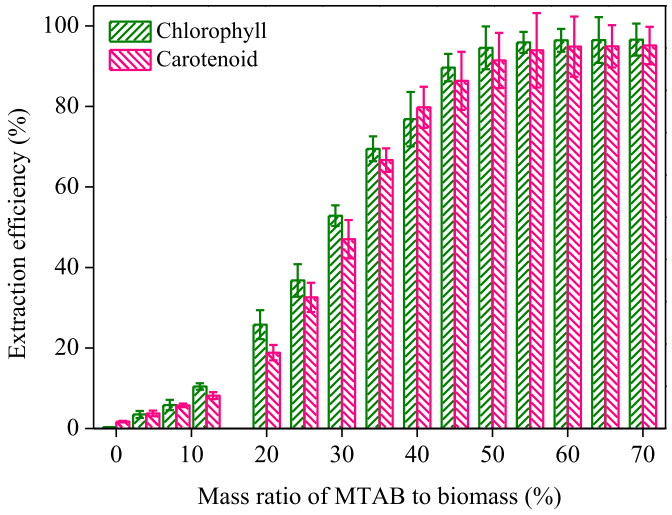

Fig. 2. Extraction efficiency of chlorophyll and carotenoid from *Synechocystis* after treatment with MTAB at various MTAB/Biomass % ratios for 180 min.

MTAB/Biomass % ratio. This increase means that the surfactant effect of MTAB was releasing EPS from the cells and converting it to components detected as soluble after centrifugation (Zhou et al., 2016a). In Stage II (from 40% to 70%), SP and SC increased dramatically, with the concentration of SP + SC having a steeper and nearly linear relationship ($R^2 = 0.995$, $P < 0.01$) with the MTAB/Biomass % ratio. The large increase in slope is a sign of cell lysis and release of intracellular soluble organics (Zhou et al., 2016a).

3.4. Flow cytometry analysis of Synechocystis

Fig. 4(a) shows FC selected results for light scattering alone for *Synechocystis* after treatment for 3 h with MTAB at the noted MTAB/

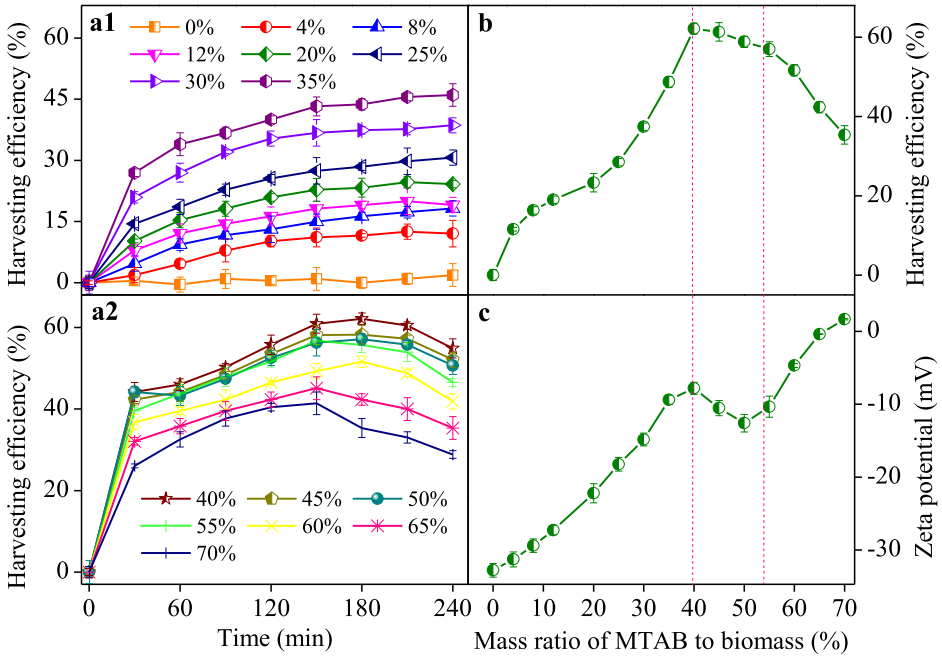

Fig. 1. (a) Time course of harvest efficiency of *Synechocystis* after treatment with MTAB at various MTAB/Biomass % ratios (legend), (b) harvest efficiency after 180 min at various MTAB/Biomass % ratios (x-axis) and (c) zeta potential of *Synechocystis* after 180 min at various MTAB/Biomass % ratios (x-axis). The vertical dashed lines in panels (b) and (c) delineate Ranges I, II, and III.

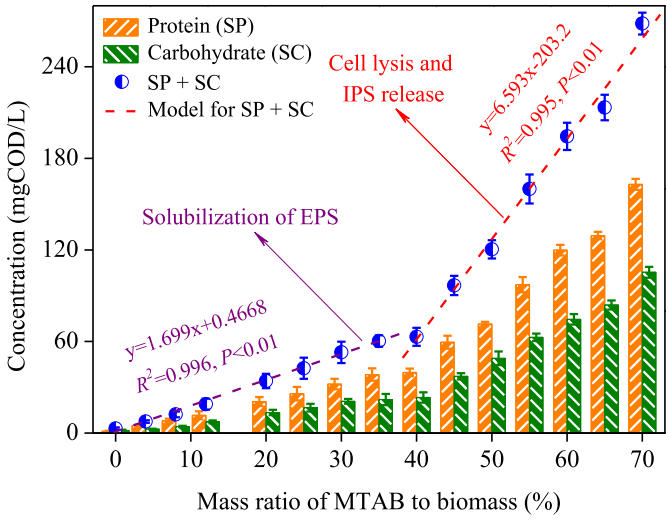

Fig. 3. Releasing of soluble protein and carbohydrate from *Synechocystis* after treatment with MTAB at various MTAB/Biomass % ratios for 180 min.

Biomass % ratios. Fig. S5 presents all the FC results for light scattering alone after treatment for 3 h with MTAB at the noted MTAB/Biomass ratios, and Fig. S4 presents the FC results for light scattering alone, fluorescence characteristics, and fluorescence intensity of NA-complexed SG of *Synechocystis* without MTAB treatment. Fig. 4(b) shows the relationship between the MTAB/biomass % ratio and the slope (SL) between the forward scatter (FSC, horizontal axis) and side scatter (SSC, vertical axis) in the region with the highest density of points.

It has been demonstrated that a decrease in SL corresponds on an increase in particle size (Hyka et al., 2013), such as by cell aggregation and the loss of EPS caused the increase of SL (Zhou et al., 2016a). Fig. 4(b) shows that MTAB significantly affected the biomass's particle size, as SL changed systematically with MTAB/Biomass % ratios. The systematic changes can be separated into three phases. In Phase I (from 0% to 8%), SL values gradually decreased with a strong linear relationship ($R^2 = 0.985$, $P < 0.01$) with MTAB/Biomass % ratio. This decrease in SL indicates cell aggregation, because MTAB neutralized surface charge and formed inter-particle bridges (Sengco et al., 2001). In Phase II (from 12% to 40%), SL increased with a strong linear relationship ($R^2 = 0.996$,

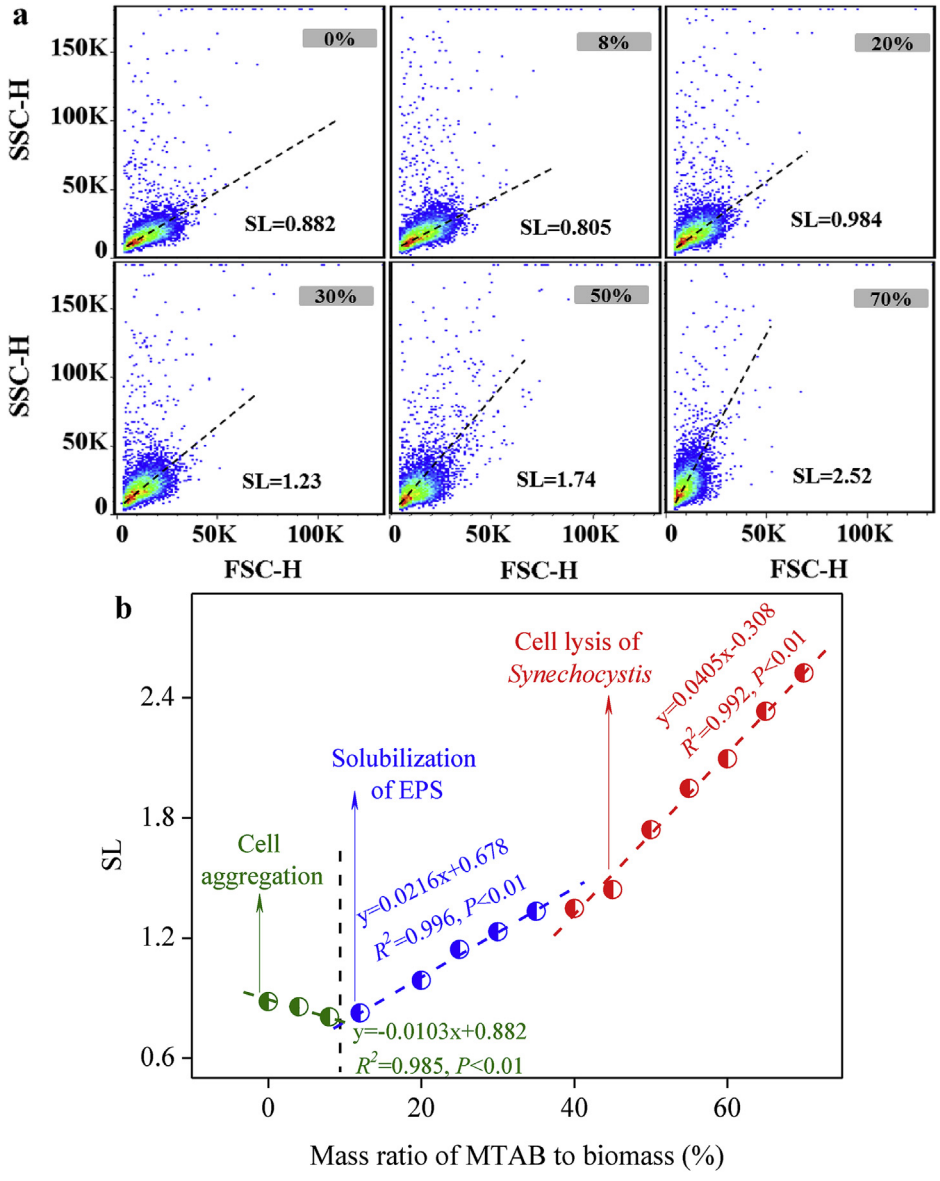

Fig. 4. (a) Selected FC results for light scattering alone of *Synechocystis* after treatment for 180 min with MTAB at the noted MTAB/Biomass ratios (legend values) and (b) relationship between the SL and the MTAB/biomass % ratio. SL, the slope of the linear relationship between FSC and SSC, is inversely related to particle size.

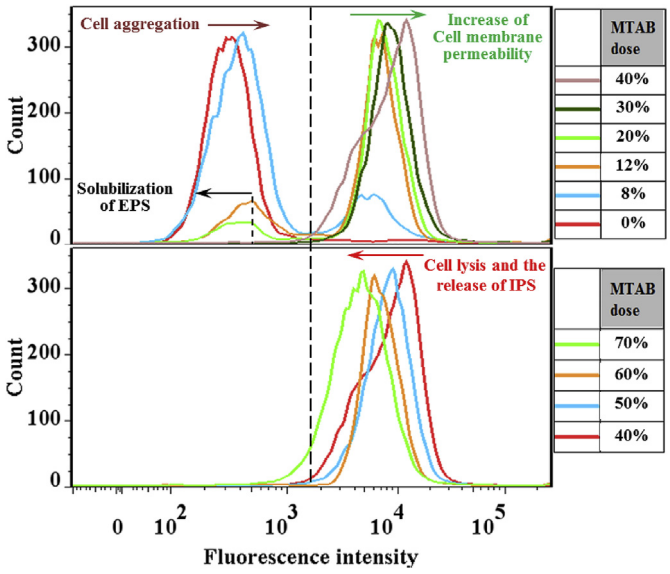

Fig. 5. Fluorescence spectra of *Synechocystis* after treatment for 180 min with MTAB at various MTAB/Biomass % ratios.

$P < 0.01$) with MTAB/Biomass % ratios. This increase in SL indicates a decrease of particle size due to the release (and solubilization) of EPS(Zhou et al., 2016a). Finally, SL dramatically increased in Phase III (from 40% to 70%), indicating a sharp decrease in particle size, which corroborates the SP and SC data (from Fig. 3) that cell lysis was occurring.

Fig. 5 presents typical fluorescence spectra of *Synechocystis* after treatment with various doses of MTAB for 3 h. Fig. S6 shows the fluorescence characteristics of *Synechocystis*; Fig. S7 gives the full fluorescence spectra and the distribution of SG emission intensity. The spectra in Fig. 5 correspond to the FC trends in Fig. S6, and they identify changes in cell-membrane permeability. As the MTAB dose increased from 0% to 8%, the peak in the low fluorescence intensity (FI) region (left of the dashed line) shifted only slightly to right. As fluorescence in the low-FI region was from the binding of SG with extracellular NA naturally in *Synechocystis* EPS (Roth et al., 1997; Zhou et al., 2016a), the slight increase of particle FI represents an increase in localized EPS concentration due to cell aggregation. When the MTAB dose increased from 12% to 40%, the peak in low FI region dramatically decreased, disappearing as the MTAB dose increased above 20%. This loss of signal in the low-FI region corresponds to the release and solubilization of EPS. In parallel, a second peak formed in the high-FI region (right of the dashed line), and that peak shifted to right with higher MTAB dose. The second peak and its steady increase signify that MTAB led to higher cell-membrane permeability (Collier, 2000; Foladori et al., 2010), which allowed SG to pass through the membrane and bind with intracellular NA. When the MTAB dose was higher than 40%, the peak in high FI region gradually shifted to left, a signal of increasing cell lysis and the resulting loss of NA inside the cells (Karp, 1979; Zipper et al., 2004).

3.5. Synthesizing the results

Fig. 6 synthesizes the results in terms of the mechanisms acting to enhance harvesting and extraction. Microscopic images of *Synechocystis* after treatment with various doses of MTAB for 3 h, presented in Fig. 7, reinforce the mechanistic interpretations.

- At low doses ($\leq$ 8%), MTAB mainly brought about coagulation and flocculation via charge neutralization and inter-particle bridging, which caused aggregation that improved biomass harvest efficiency (Fig. 2). Microscopy in Fig. 7 illustrates this well in the 4% and 8% panels.
- Adding more MTAB, up to 40%, released and solubilized EPS via its surfactant action (Figs. 3 and 4). EPS release lowered gave the biomass an increasingly less negative charge (Fig. 2 (c)), but also led to break up of the large aggregates back into small particles; Fig. 7's 12% and 20% panels show the disaggregation. The increase of cell permeability in this stage allowed EA to pass into the cells and extract pigments more effectively (Fig. 5). Complete EPS removal, but with minimal cell lysis, minimized the surface negative charge of biomass and achieved the maximum harvest efficiency.
- Even more MTAB (> 40%) led to cell lysis and a large increase in soluble organics (Fig. 3), which left cell shells and debris in the culture, which is seen clearly in Fig. 7's 60% and 70% panels. While, the extraction efficiency remained stable with an MTAB dose higher than 60% (Fig. 2), cell lysis increased (Figs. 3–5), which means that complete cell lysis was not required to achieve the maximum extraction efficiency. The treatment giving the maximum extraction efficiency released only about 20% of the intracellular protein + carbohydrate (Fig. 3).

For environmentally sustainable development, the indiscriminate discharge of surfactant-containing wastewater after biomass harvesting and pigments extraction is not acceptable due to its toxicity to humans and the environment. Additionally, recycling the culture water containing surfactant for the biomass cultivation could adversely affect microalga growth. In this study, we selected a biodegradable cationic surfactant (Bergero and Lucchesi, 2013; Hajaya and Pavlostathis, 2012); in addition, a previous study (Lai et al., 2017) has demonstrated continuous biodegradation of a set of quaternary ammonium compound (QAC) using an oxygen-based membrane biofilm reactor (O_2-MBfR) with an influent QAC concentration up to 400 mg/L. Bubbleless O_2 transfer completely eliminated foaming, and biofilm accumulation helped the QAC biodegraders resist toxicity. Thus, biodegradation of MTAB and

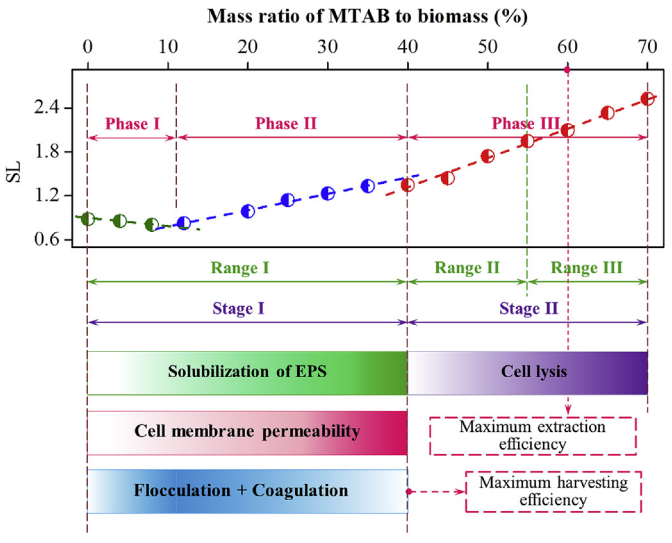

Fig. 6. Synthesis of mechanisms acting to enhance biomass harvesting and pigment extraction from *Synechocystis* after treatment with MTAB. A deeper color in a bar signifies an increase of the mechanism with MTAB dose. White color means that the mechanism is not in effect. (For interpretation of the references to colour in this figure legend, the reader is referred to the web version of this article.)

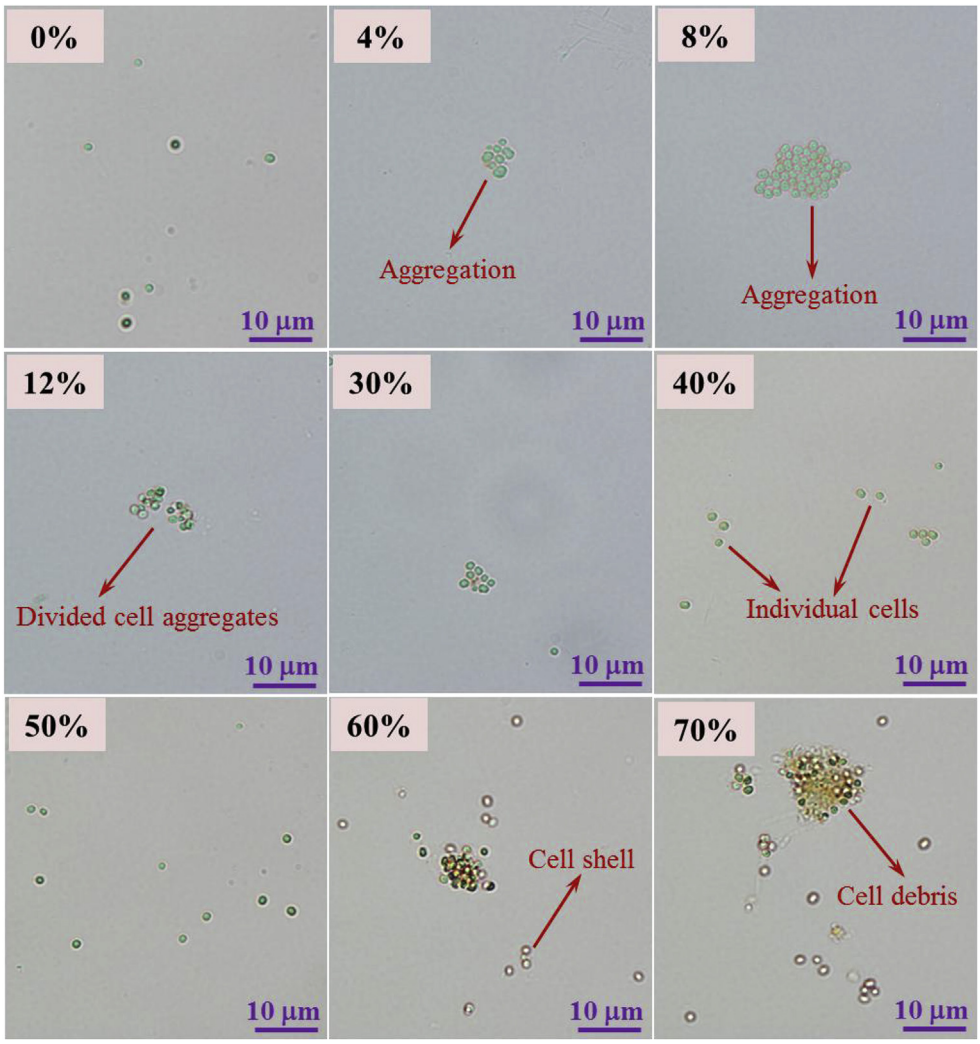

Fig. 7. Microscopic images of *Synechocystis* after MATB treatment for 180 min at the noted MTAB/Biomass % ratios. Noted are examples of cell aggregation, divided cell aggregates (disaggregation), individual cells, shells of lysed cells, and cell debris.

similar QACs should prevent their discharge to aquatic environments.

4. Conclusions

Development of efficient biomass-harvesting and pigments-extraction technologies for microalgae may yield major cost and energy savings in large-scale utilization of microalgae biomass and the key step should be explored the mechanisms systematically. Our study emphasizes the mechanisms by which MTAB enhances biomass harvesting and pigments extraction from *Synechocystis*. At a low dose ($\leq$ 8%), MTAB mainly brought about coagulation and flocculation, which led to aggregation that improved harvesting. MTAB dose from 8% to 40% released and solubilized EPS, which lowered the biomass's negative charge, but also led to the breakup of the large aggregates. The increase of cell permeability in this stage allowed EA to pass into the cells and achieve better pigment extraction. Even more MTAB (> 40%) led to cell lysis and a large increase in soluble organics. With a MTAB/Biomass % ratio of 40%, complete EPS removal was achieved with minimal cell lysis, yielding a maximum harvest efficiency of 62%. Pigment extraction plateaued at > 90% recovery for MTAB/Biomass % ratios of greater than 50%, indicating that complete cell lysis was not required to achieve the maximum extraction efficiency. The MTAB/Biomass % ratio for optimizing harvest efficiency and pigment extraction lay in the range of 40%–60%. Doses closer to 40% favor harvest efficiency, while doses closer to 60% favor pigment extraction. This work lays the foundation for optimizing surfactant dose for biomass harvesting and pigment extraction.

Acknowledgments

This work was supported in part by LightWorks, Arizona State University, and in part by China Scholarship Council (NO.201506260022), National Science Foundation of China (51678422, 51378368), the National Key Project of Research and Development Plan of China (No. 2017YFC0403403), and Shanghai Tongji Gao Tingyao Environmental Science & Technology Development Foundation. We thank Dr. Dong Fu, Biodesign Center of Infectious Diseases and Vaccinology, Arizona State University, for her expertise in flow cytometry for sample quantification; and Dr. Willem Vermaas and his laboratory in the School of Life Sciences at Arizona State University for providing *Synechocystis* sp. PCC6803 wild type.

Appendix A. Supplementary data

Supplementary data related to this article can be found at

https://doi.org/10.1016/j.watres.2017.09.036.

References

Association, A.P.H., 1998. Standard Methods for the Examination of Water and Wastewater. American Public Health Association, Washington, DC, p. 1268.

Ayed, H.B.A.-B., Taidi, B., Ayadi, H., Pareau, D., Stambouli, M., 2015. Effect of magnesium ion concentration in autotrophic cultures of Chlorella vulgaris. Algal Res. 9, 291–296.

Bergero, M.F., Lucchesi, G.I., 2013. Degradation of cationic surfactants using Pseudomonas putida A ATCC 12633 immobilized in calcium alginate beads. Biodegradation 24 (3), 353–364.

Biggs, S., Habgood, M., Jameson, G.J., 2000. Aggregate structures formed via a bridging flocculation mechanism. Chem. Eng. J. 80 (1), 13–22.

Collier, J.L., 2000. Flow cytometry and the single cell in phycology. J. Phycol. 36 (4), 628–644.

Foladori, P., Tamburini, S., Bruni, L., 2010. Bacteria permeabilisation and disruption caused by sludge reduction technologies evaluated by flow cytometry. Water Res. 44 (17), 4888–4899.

Frølund, B., Palmgren, R., Keiding, K., Nielsen, P.H., 1996. Extraction of extracellular polymers from activated sludge using a cation exchange resin. Water Res. 30 (8), 1749–1758.

Gilbert-López, B., Mendiola, J.A., Fontecha, J., van den Broek, L.A.M., Sijtsma, L., Cifuentes, A., Herrero, M., Ibáñez, E., 2015. Downstream processing of Isochrysis galbana: a step towards microalgal biorefinery. Green Chem. 17 (9), 4599–4609.

Hajaya, M.G., Pavlostathis, S.G., 2012. Fate and effect of benzalkonium chlorides in a continuous-flow biological nitrogen removal system treating poultry processing wastewater. Bioresour. Technol. 118, 73–81.

Hermansson, M., 1999. The DLVO theory in microbial adhesion. Colloids. Surfaces B Biointerfaces 14 (1), 105–119.

Hyka, P., Lickova, S., Přibyl, P., Melzoch, K., Kovar, K., 2013. Flow cytometry for the development of biotechnological processes with microalgae. Biotechnol. Adv. 31 (1), 2–16.

Karp, G., 1979. Cell Biology. McGrawHill, New York.

Lai, Y.S., De Francesco, F., Aguinaga, A., Parameswaran, P., Rittmann, B.E., 2016a. Improving lipid recovery from Scenedesmus wet biomass by surfactant-assisted disruption. Green Chem. 18 (5), 1319–1326.

Lai, Y.S., Ontiveros-Valencia, A., Ilhan, Z.E., Zhou, Y., Miranda, E., Maldonado, J., Krajmalnik-Brown, R., Rittmann, B.E., 2017. Enhancing biodegradation of C16-alkyl quaternary ammonium compounds using an oxygen-based membrane biofilm reactor. Water Res. 123, 825–833.

Lai, Y.S., Zhou, Y., Martarella, R., Wang, Z., Rittmann, B.E., 2016b. Synergistic integration of C12–C16 cationic surfactants for flocculation and lipid extraction from Chlorella biomass. ACS Sustain. Chem. Eng. 5 (1), 752–757.

Lebaron, P., Catala, P., Parthuisot, N., 1998. Effectiveness of SYTOX Green stain for bacterial viability assessment. Appl. Environ. Microbiol. 64 (7), 2697–2700.

Li, Y., Xu, Y., Zheng, T., Wang, H., 2017. Flocculation mechanism of the actinomycete Streptomyces sp. hsn06 on Chlorella vulgaris. Bioresour. Technol. 239, 137–143.

Liu, X.-M., Sheng, G.-P., Yu, H.-Q., 2007. DLVO approach to the flocculability of a photosynthetic H2-producing bacterium, Rhodopseudomonas acidophila. Environ. Sci. Technol. 41 (13), 4620–4625.

Lu, Y., Zheng, G., Wu, W., Cui, C., Zhou, L., 2017. Significances of deflocculated sludge flocs as well as extracellular polymeric substances in influencing the compression dewatering of chemically acidified sludge. Sep. Purif. Technol. 176, 243–251.

Magara, Y., Nambu, S., Utosawa, K., 1976. Biochemical and physical properties of an activated sludge on settling characteristics. Water Res. 10 (1), 71–77.

Nguyen, B.T., Rittmann, B.E., 2016. Effects of inorganic carbon and pH on growth kinetics of *Synechocystis* sp. PCC 6803. Algal Res. 19, 363–369.

Nguyen, B.T., Rittmann, B.E., 2015. Predicting dissolved inorganic carbon in photoautotrophic microalgae culture via the nitrogen source. Environ. Sci. Technol. 49 (16), 9826–9831.

Oswald, W.J., Golueke, C.G., 1960. Biological transformation of solar energy. Adv. Appl. Microbiol. 2, 223–262.

Pittman, J.K., Dean, A.P., Osundeko, O., 2011. The potential of sustainable algal biofuel production using wastewater resources. Bioresour. Technol. 102 (1), 17–25.

Ries, H.E., Meyers, B.L., 1968. Flocculation mechanism: charge neutralization and bridging. Science 160 (3835), 1449–1450.

Rippka, R., Deruelles, J., Waterbury, J.B., Herdman, M., Stanier, R.Y., 1979. Generic assignments, strain histories and properties of pure cultures of cyanobacteria. Microbiology 111 (1), 1–61.

Rittmann, B.E., McCarty, P.L., 2001. Environmental Biotechnology: Principles and Applications. McGrawHill, New York, p. 400.

Roth, B.L., Poot, M., Yue, S.T., Millard, P.J., 1997. Bacterial viability and antibiotic susceptibility testing with SYTOX green nucleic acid stain. Appl. Environ. Microbiol. 63 (6), 2421–2431.

Ruiz, J., Olivieri, G., de Vree, J., Bosma, R., Willems, P., Reith, J.H., Eppink, M.H.M., Kleinegris, D.M.M., Wijffels, R.H., Barbosa, M.J., 2016. Towards industrial products from microalgae. Energy. Environ. Sci. 9 (10), 3036–3043.

Salim, S., Bosma, R., Vermuë, M.H., Wijffels, R.H., 2011. Harvesting of microalgae by bio-flocculation. J. Appl. Phycol. 23 (5), 849–855.

Schott, H., Kwan, L.C., Feldman, S., 1982. The role of surfactants in the release of very slightly soluble drugs from tablets. J. Pharm. Sci. 71 (9), 1038–1045.

Schwarz, A.O., Rittmann, B.E., 2007. A biogeochemical framework for metal detoxification in sulfidic systems. Biodegradation 18 (6), 675–692.

Sengco, M.R., Li, A., Tugend, K., Kulis, D., Anderson, D.M., 2001. Removal of red-and brown-tide cells using clay flocculation. I. Laboratory culture experiments with Gymnodinium breve and Aureococcus anophagefferens. Mar. Ecol. Prog. Ser. 210, 41–53.

Seo, J.Y., Praveenkumar, R., Kim, B., Seo, J.-C., Park, J.-Y., Na, J.-G., Jeon, S.G., Park, S.B., Lee, K., Oh, Y.-K., 2016. Downstream integration of microalgae harvesting and cell disruption by means of cationic surfactant-decorated Fe 3 O 4 nanoparticles. Green Chem. 18 (14), 3981–3989.

Sheng, J., Vannela, R., Rittmann, B.E., 2011. Evaluation of cell-disruption effects of pulsed-electric-field treatment of Synechocystis PCC 6803. Environ. Sci. Technol. 45 (8), 3795–3802.

Vandamme, D., Foubert, I., Muylaert, K., 2013. Flocculation as a low-cost method for harvesting microalgae for bulk biomass production. Trends Biotechnol. 31 (4), 233–239.

Vermes, I., Haanen, C., Reutelingsperger, C., 2000. Flow cytometry of apoptotic cell death. J. Immunol. Methods 243 (1), 167–190.

Wan, C., Alam, M.A., Zhao, X.-Q., Zhang, X.-Y., Guo, S.-L., Ho, S.-H., Chang, J.-S., Bai, F.-W., 2015. Current progress and future prospect of microalgal biomass harvest using various flocculation technologies. Bioresour. Technol. 184, 251–257.

Zhang, Z., Zhou, Y., Zhang, J., Xia, S., Hermanowicz, S.W., 2016. Effects of short-time aerobic digestion on extracellular polymeric substances and sludge features of waste activated sludge. Chem. Eng. J. 299, 177–183.

Zhou, Y., Nguyen, B.T., Lai, Y.S., Zhou, C., Xia, S., Rittmann, B.E., 2016a. Using flow cytometry to evaluate thermal extraction of EPS from Synechocystis sp. PCC 6803. Algal Res. 20, 276–281.

Zhou, Y., Xia, S., Zhang, J., Nguyen, B.T., Zhang, Z., 2017a. Insight into the influences of pH value on Pb (II) removal by the biopolymer extracted from activated sludge. Chem. Eng. J. 308, 1098–1104.

Zhou, Y., Xia, S., Zhang, Z., Zhang, J., Hermanowicz, S.W., 2016b. Associated adsorption characteristics of Pb (II) and Zn (II) by a novel biosorbent extracted from waste-activated sludge. J. Environ. Eng. 142 (7), 04016032.

Zhou, Y., Zhang, J., Zhang, Z., Zhou, C., Lai, Y.S., Xia, S., 2017b. Enhanced performance of short-time aerobic digestion for waste activated sludge under the presence of cocoamidopropyl betaine. Chem. Eng. J. 320, 494–500.

Zhou, Y., Zhang, Z., Zhang, J., Xia, S., 2016c. Understanding key constituents and feature of the biopolymer in activated sludge responsible for binding heavy metals. Chem. Eng. J. 304, 527–532.

Zipper, H., Brunner, H., Bernhagen, J., Vitzthum, F., 2004. Investigations on DNA intercalation and surface binding by SYBR Green I, its structure determination and methodological implications. Nucleic acids Res. 32 (12) e103–e103.